

Mean-square displacement from Mössbauer and x-ray data for solid krypton: A comparison of theory and experiment

R. C. Shukla

Department of Physics, Brock University, St. Catharines, Ontario, Canada L2S 3A1

D. W. Taylor

Department of Physics, McMaster University, Hamilton, Ontario, Canada L8S 4M1

(Received 3 September 1993)

The Mössbauer recoilless fraction is calculated from the lowest-order anharmonic-perturbation theory, the Green's-function method, which sums the lowest-order anharmonic contributions to all orders, and the Monte Carlo method. In all cases we have employed a nearest-neighbor-interaction Lennard-Jones and Morse potential. Excellent agreement is shown to exist between the theory and the Mössbauer and x-ray experimental results.

The recoilless Mössbauer fraction f of ^{83}Kr in solid Kr was measured as a function of temperature by Gilbert and Violet¹ (GV). The experimental values of f by GV for the 9.4 KeV transition of ^{83}Kr in solid Kr were evaluated again by Kolk² using a nuclear resonance cross section $\sigma_0 = (1.15 \pm 0.03) \times 10^{-18} \text{ cm}^2$. Kolk's work was prompted because the experimental values of f as determined by GV were much lower than those calculated from the Debye-type harmonic theory³ and some approximate anharmonic theories.^{4,5}

The purpose of this work is to calculate f from a variety of theoretical methods now available in the literature⁶⁻⁸ for inclusion of the anharmonic effects and then compare them with the revised f values of Kr as determined by Kolk.^{2,9}

We have employed the following methods in our calculations of f for Kr, viz., the lowest-order (λ^2) anharmonic perturbation theory (PT),^{6,8} the Green's-function method⁷ and the Monte Carlo (MC) method.⁶ The latter two methods include anharmonic contributions to all orders of anharmonicity with the qualification that only certain types of anharmonic contributions arising from the cubic and quartic terms of the anharmonic Hamiltonian are included in the Green's-function method. Since the calculation by these three methods can be carried out quite accurately it is worthwhile to make a comparison of the theoretical results for f from each of these methods with the experimental values. We believe this to be an accurate anharmonic calculation of f for Kr. Since the experimental data are known in the low-temperature range up to 85 K we compute the quasiharmonic contribution from the finite temperature expression for the mean-square atomic displacement (MSD), $\langle u^2 \rangle$, and calculate the lowest-order (λ^2) anharmonic contributions to MSD in the high-temperature limit ($T > \Theta_D$, Θ_D is the Debye temperature). The λ^2 contributions are added as corrections to the quasiharmonic result in the temperature range $\Theta_D \leq T \leq T_m$, where T_m is the melting temperature. In all three calculations mentioned above we use the nearest-neighbor central force model of the fcc lattice with atoms interacting via the 6-12 Lennard-Jones (LJ)

interaction potential and the Morse Potential, with parameters given in Shukla and Shanes.¹⁰

The $\langle u^2 \rangle$ results from the Green's-function method⁷ are obtained from the following:

$$\langle u^2 \rangle = \frac{k_B T}{NM} \sum_{\mathbf{q}, j} \frac{1}{\Omega_{\mathbf{q}j}^2}, \quad (1)$$

$$\Omega_{\mathbf{q}j}^2 = \omega_{\mathbf{q}j}^2 + \Delta_3(\mathbf{q}j) + \Delta_4(\mathbf{q}j), \quad (2)$$

$$\begin{aligned} \Omega_{\mathbf{q}j}^2 = \omega_{\mathbf{q}j}^2 - \frac{\lambda^2}{2\beta N} \sum_{\mathbf{q}_1 j_1} \sum_{\mathbf{q}_2 j_2} \Delta(\mathbf{q}_1 + \mathbf{q}_2 + \mathbf{q}) \\ \times \frac{|\Phi(\mathbf{q}_1 j_1, \mathbf{q}_2 j_2, \mathbf{q}j)|^2}{\omega_{\mathbf{q}_1 j_1}^2 \omega_{\mathbf{q}_2 j_2}^2} \\ + \frac{\lambda^2}{2\beta N} \sum_{\mathbf{q}_1 j_1} \frac{\Phi(\mathbf{q}_1 j_1, -\mathbf{q}_1 j_1, \mathbf{q}j, -\mathbf{q}j)}{\omega_{\mathbf{q}_1 j_1}^2}, \end{aligned} \quad (3)$$

whereas the high-temperature limit quasiharmonic and the λ^2 anharmonic contributions are calculated from⁸

$$2M_{\text{QH}} = \frac{|\mathbf{q}|^2 3k_B T}{6B(r)} S_{\text{QH}}(a_1), \quad (4)$$

$$\begin{aligned} 2M_1(\mathbf{q}) = - \frac{|\mathbf{q}|^2 (k_B T)^2}{3B^3(r)} \left[D(r) S_{4A}(a_1) \right. \\ \left. + \frac{C(r)}{r} S_{4B}(a_1) \right. \\ \left. + \frac{B(r)}{r^2} S_{4C}(a_1) \right], \end{aligned} \quad (5)$$

$$\begin{aligned} 2M_2(\mathbf{q}) = \frac{|\mathbf{q}|^2 (k_B T)^2}{F^4(r)} \left[C^2(r) S_{3A}(a_1) \right. \\ \left. + \frac{2B(r)C(r)}{r} S_{3B}(a_1) \right. \\ \left. + \frac{B^2(r)}{r^2} S_{3C}(a_1) \right], \end{aligned} \quad (6)$$

and finally the quasiharmonic contribution to MSD in the low-temperature range is calculated from the following finite temperature expression:

$$2M_{\text{QH}} = \frac{|\mathbf{q}|^2}{3} \frac{\hbar}{2NM} \sum_{\mathbf{q}j} \frac{(2n_{\mathbf{q}j} + 1)}{\omega_{\mathbf{q}j}}. \quad (7)$$

The MSD is related to $2M$ via $2M = (|\mathbf{q}|^2/3)\langle u^2 \rangle$ and the Mössbauer fraction is given by $f = \exp[-2M]$.

In Eqs. (1)–(7) the various symbols have the following meaning: \hbar is the Planck's constant divided by 2π ; N represents the number of unit cells in the crystal and M the atomic mass; T is the temperature and k_B the Boltzmann constant and $\beta = (k_B T)^{-1}$; $\omega_{\mathbf{q}j}$ is the phonon frequency for the wave vector \mathbf{q} and branch index j ; $\Omega_{\mathbf{q}j}$ is the renormalized phonon frequency which is calculated from Eq. (2) with the knowledge of the cubic shift $\Delta_3(\mathbf{q}j)$ and quartic shift $\Delta_4(\mathbf{q}j)$ whose expressions are obtained from the second and third terms, respectively, on the right-hand side of Eq. (3). The Φ functions in Eq. (3) are the Fourier transforms of the third and fourth rank tensors. Full details of the calculation can be obtained from Ref. 7. B , C , D in Eqs. (4)–(6) are given by

$$B = \left[\frac{1}{r} \frac{d}{dr} \right]^2 \phi(r), \quad C = \left[\frac{1}{r} \frac{d}{dr} \right]^3 \phi(r),$$

$$D = \left[\frac{1}{r} \frac{d}{dr} \right]^4 \phi(r),$$

where $\phi(r)$ is a two-body potential function and $F(r) = \phi''(r) + (1/r)\phi'$ with primes denoting the corresponding derivatives of ϕ . The functions $S_{\text{QH}}(a_1)$, $S_{4A}(a_1)$, $S_{3A}(a_1)$, and similar other functions in Eqs. (4)–(6) represent the various Brillouin zone (BZ) sums which arise in the quasiharmonic and the λ^2 anharmonic calculations of MSD. In Ref. 8, these sums were evaluated to a high degree of accuracy and fitted to an exponential function involving polynomials of degree 5 in the form $f(a_1) = \exp[P(a_1)]$, where $P(a_1) = \sum_{n=0}^5 b_n (a_1)^n$. The coefficients b_n for these polynomials are given in Ref. 8 in Table IV. a_1 is a parameter which characterizes the volume dependence of the Brillouin-zone sums. It is defined by $a_1 = \phi' / [r\phi'' - \phi']$. Full details of these calculations can be obtained from Ref. 8.

Although in Ref. 8 the quasiharmonic (S_{QH}) and the quartic BZ sums (S_{4A} , etc.) have been calculated very accurately, we find that there is some room for improvement in the cubic BZ sums. Hence we present in Table I the revised values of S_{3A} , S_{3B} , and S_{3C} for different values of a_1 in $0 \leq a_1 \leq 0.1$ at intervals of 0.02. In calculating these values we have used the scanning procedure and evaluated them for a mesh of odd and even wave vectors for step lengths 10, 20, and 30. Here the step length is defined as the number of steps from the origin to the boundary of the BZ in the x direction. The values presented in Table I are the extrapolated values for the infinite step length. These values of S_{3A} , S_{3B} , and S_{3C} are about 5% higher than those presented in Shukla and Plint.⁸ In order to have a check on our numerical results,

TABLE I. Dimensionless sums S_{3A} , S_{3B} , and S_{3C} for different values of a_1 .

a_1	S_{3A}	S_{3B}	S_{3C}
0.10	0.029 753 7	0.104 224	0.580 168
0.08	0.032 320 3	0.112 772	0.631 239
0.06	0.035 517 8	0.123 387	0.695 066
0.04	0.039 590 6	0.136 864	0.776 690
0.02	0.044 922 2	0.154 427	0.884 089
0.00	0.052 1420	0.178 088	1.030 54

the finite-temperature quasiharmonic contribution was evaluated in the temperature range $5 \text{ K} \leq T \leq 60 \text{ K}$ by two procedures: (1) by a straightforward sampling procedure with a regular cubic mesh, and (2) by the Gilat-Raubenheimer method for the calculation and subsequent integration purposes involving the phonon distribution function $g(\omega)$. They agreed to four significant figures.

As mentioned earlier, the high-temperature results from the λ^2 contribution were added to the above quasiharmonic results for $T > \Theta_D$, where Θ_D was chosen as 64 K.¹¹ In Fig. 1 we present these results for f along with the experimentally determined Mössbauer and x-ray results. The x-ray results have been determined by Windecker,¹² and Mössbauer by Kolk.^{2,9} The MC results are also presented in this figure.

In Fig. 2 we have presented the high-temperature results for the λ^2 contribution, the Green's-function method (shown as RE—renormalized frequencies) and the MC method. The lattice spacings for all three methods are the same as given by the zero-pressure condition in the MC method. They are given in Ref. 13.

In Fig. 3 we present the result for the Morse potential from the experimentally determined lattice spacings for the finite-temperature quasiharmonic case with the λ^2 corrections added to them in the high-temperature limit. The experimental values are again from the Mössbauer and x-ray sources.

The experimental values for $\ln f$ shown in Figs. 1 and 3

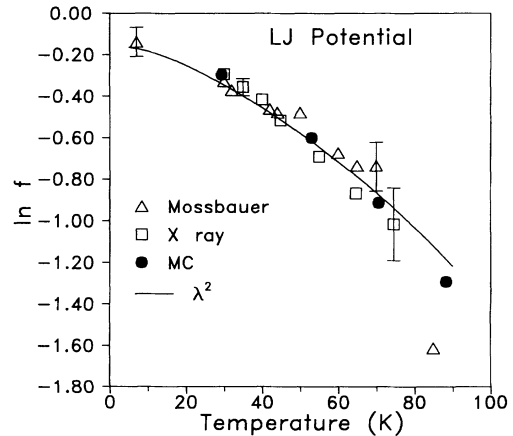


FIG. 1. Mössbauer fraction in Kr (represented as $\ln f$) versus temperature. Squares are the x-ray results, triangles are the Mössbauer results. For the LJ potential, black dots and the solid line represent the MC and the λ^2 PT results, respectively.

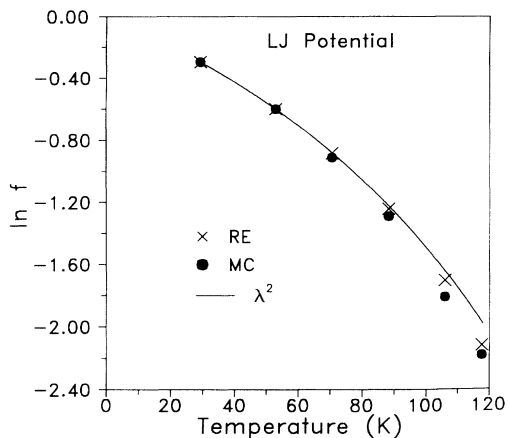


FIG. 2. Mössbauer fraction in Kr (represented as $\ln f$) versus temperature for the LJ potential in the high-temperature limit. Crosses are the Green's-function (RE) results, black dots and the solid line represent the MC and the λ^2 PT results, respectively.

that are labeled Mössbauer, are based on the experimental work of Gilbert and Violet.^{1,14} The value of the internal conversion coefficient available to Gilbert and Violet was not correct and Kolk^{2,9} has reanalyzed the experimental data using a later value of the internal conversion coefficient. We have used the more recent analysis of Kolk⁹ which is less sensitive to the physical parameters used in the analysis. It gives larger values of $\ln f$ than his earlier analysis. Note the value of 85 K. This was incorrectly placed at 80 K in Fig. 2 of Kolk,⁹ there being no data for 80 K in Gilbert's thesis.¹⁴ The x-ray values of $\ln f$ in Figs. 1 and 3 are due to Windecker¹² and have been read off Fig. 1 of Kolk.² Representative values for the uncertainties in $\ln f$ also shown in Figs. 1 and 3. The uncertainties in the Mössbauer values are approximately the same for all temperatures, where the uncertainties in the x-ray values increase with temperature.

It is clear from these results that for both potentials

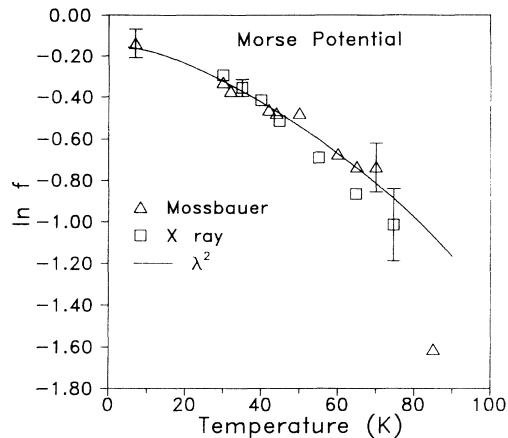


FIG. 3. Mössbauer fraction in Kr (represented as $\ln f$) versus temperature for the Morse potential. The figure legends are the same as in Fig. 1.

with experimental lattice spacings¹⁵ the agreement between the theory and experiment is quite good in the temperature range $5 \text{ K} \leq T \leq 85 \text{ K}$, although the LJ results are a shade better than the Morse results. The experimental point at 85 K is taken from Gilbert's thesis. In comparison to other experimental points this seems to be very low. Since no experimental data is available above 85 K the theoretical results cannot be tested in the temperature range $85 \text{ K} \leq T \leq 116 \text{ K}$. Within the range of experimental measurements with respect to temperature it is difficult to distinguish the results of the three theories presented in Fig. 2. The results of three theories differ from each other for $T > 100 \text{ K}$. A measurement in this temperature range is highly desirable for testing anharmonic theories.

The authors wish to acknowledge the support of the Natural Sciences and Engineering Research Council of Canada.

¹K. Gilbert and C. E. Violet, *Phys. Lett.* **28A**, 285 (1968).

²B. Kolk, *Phys. Lett.* **35A**, 83 (1971).

³K. Mahesh, *J. Phys. Soc. Jpn.* **28**, 818 (1970).

⁴J. S. Brown, *Phys. Rev.* **187**, 401 (1969).

⁵J. S. Brown, *Phys. Rev. B* **3**, 21 (1971).

⁶G. A. Heiser, R. C. Shukla, and E. R. Cowley, *Phys. Rev. B* **33**, 2158 (1986).

⁷R. C. Shukla and Herman Hübschle, *Phys. Rev. B* **40**, 1555 (1989).

⁸R. C. Shukla and C. A. Plint, *Phys. Rev. B* **40**, 10337 (1989).

⁹B. Kolk, *Phys. Rev. B* **12**, 4695 (1975).

¹⁰R. C. Shukla and F. Shanes, *Phys. Rev. B* **32**, 2513 (1985).

¹¹B. M. Powell and G. Dolling, in *Rare Gas Solids*, edited by M. L. Klein and J. A. Venables (Academic, New York, 1976), Vol. II.

¹²R. C. Windecker, Ph.D. thesis, University of Illinois, Urbana, Illinois, 1970.

¹³E. R. Cowley, *Phys. Rev. B* **28**, 3160 (1983).

¹⁴K. G. Gilbert, Ph.D. thesis, University of California, 1968 (unpublished).

¹⁵P. Korpiun and E. Lüscher, in *Rare Gas Solids* (Ref. 11).